PHYSICAL REVIEW B **71**, 245305 (2005)

Collective behavior of single electron effects in a single layer Si quantum dot array at room temperature

L. W. Yu, K. J. Chen,* L. C. Wu, M. Dai, W. Li, and X. F. Huang

National Laboratory of Solid State Microstructures and Department of Physics, Nanjing University, Nanjing 210093, China

(Received 14 November 2004; revised manuscript received 24 March 2005; published 3 June 2005)

In this paper, we report direct experimental evidence of collective single electron effects in a single layer Si quantum dot (Si-QD) array at room temperature. The unique peak structure, observed in both the *I-V* and the capacitance-voltage (*C-V*) characteristics, differs remarkably from the peaks and the staircase structures reported for the case of an individual quantum dot and reveals the collective Coulomb blockade and the quantum confinement effects in the weakly coupled Si-QD array. Simple theoretical estimations have been made to interpret the origin of the unique peak structure. Moreover, the number of charged electrons for each peak calculated from the underlying area of the peaks both in the *I-V* (after subtracting the background current) and the *C-V* characteristics is found to be consistent with the number of coupled quantum dots under the electrode. This good agreement supports the assumption that each peak in the characteristics corresponds to a collective charging process of single electron into a subband in the Si-QD array arising from the weakly interdot coupling. This collective single electron effect in Si-QD array is important for its future application in the nanoelectronic devices.

DOI: 10.1103/PhysRevB.71.245305 PACS number(s): 73.63.Kv, 73.23.Hk, 73.21.La

INTRODUCTION

Single electron tunneling and charging effects in quantum dots (QDs)[1–3] and their potential applications in single electron devices (SEDs)[4–14] have been extensively studied for more than a decade, not only as physical phenomena in nanostructures, but also as operating principles for future integrated circuit.

To date, many approaches have been employed to fabricate ultrasmall QDs in different materials for applications in devices.[7,8,15] Previously, SEDs fabricated by electron-beam lithography (EBL), called as one of the "top-down" methods, have been reported.[8] However, low throughput and high cost make it impracticable for mass production. On the other hand, self-assembled Si-QD, as a "bottom-up" approach, are considered one of the most promising candidates for the future applications, which could be exploited for inexpensive mass production of well-defined QDs with high density. Moreover, to make the nanodevices work at room temperature, the size of the dots has to be scaled down to several nanometers to guarantee the Coulomb blockade (CB) energy and quantum confinement (QC) energy to be larger than the thermal vibration energy.

Recently, for the study of the electronic properties of self-assembled Si-QDs, Baron *et al.*[15] have reported single electron effects of individual Si-QD measured by using scanning tunneling microscopy (STM). Another report on resonant tunneling through individual Si-QD obtained by conductive cantilever of atomic force microscopy (AFM), has also been presented by Fukuda *et al.*[16] Though the utilization of STM or AFM tips provides a selective and precise study on the electronic properties of the individual quantum dot from the Si-QD array, however, from the application point of view, it is particularly important and necessary to understand the electronic properties of the Si-QD array at room temperature, due to its better noise immunity against background charge.[17]

Meanwhile, the properties arising from the interdot coupling have become a hot topic.[18–22] The electron addition spectrum in arrays of coupled QDs in the Coulomb blockade regime has been studied theoretically by Stafford *et al.*[18] It is shown that in a weak interdot coupling regime, the collective Coulomb blockade still remained. More recently, the tunneling current through the coupled QD array have been studied by Kou *et al.*,[19] the formation of subbands due to the interdot coupling is discussed in a mixed Hubbard and Anderson model. However, the experimental study of the transport through a coupled Si-QD array has not been reported yet.

In this paper, we demonstrate the collective single electron effects in the single layer Si-QD array at room temperature. The Coulomb blockade and quantum confinement energies deduced from the *I-V* and the capacitance-voltage (*C-V*) curves agree well with that predicted by an orthodox quantum model.[1] Meanwhile, the interdot coupling in the Si-QD array gives rise to the formation of a subband and manifests itself in the unique peak structure in both the *I-V* and the *C-V* characteristics, which differ remarkably from those of individual QD. Furthermore, the number of states (NOS) within each subband, estimated from the number of coupled QDs under the electrode,[22] is found to be equal to the number of injected electrons for each peak, calculated from the underlying area of the peaks both in the *I-V* and the *C-V* characteristics. This agreement directly proves that collective single electron effects can be observed in the Si-QD array at room temperature.

SAMPLE FABRICATION AND MEASUREMENT

The SiO_2/Si-QD array/SiO_2 structure is fabricated on the substrates of n^+-type (0.005–0.007 Ω cm) crystalline silicon (100) in plasma enhanced chemical vapor deposition (PECVD) system at 250 °C. A tunneling SiO_2 layer (2 nm) is formed at first by plasma oxidation on silicon substrates. Subsequently, a layer of the Si-QD array is made from hydrogen-diluted silane by layer-by-layer deposition technique. Finally, a gate SiO_2 layer is made *in situ* by plasma

 ©2005 The American Physical Society

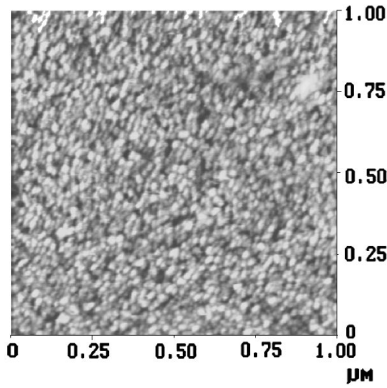

FIG. 1. A plane-view AFM image of the Si-QD array after the gate SiO_2 layer having been removed by diluted HF solution.

oxidation again under the same condition as that of the tunneling SiO_2 layer. The details on sample fabrication were reported in our previous work.[23] After that, the samples are annealed in N_2 ambient at a temperature of 900 °C for 30 min, which is essential to finally form the well-defined Si-QD,[24] and reduce the interface states and defects in the structure. Al electrodes with an area of 0.8×10^{-3} cm^2 on the topside and backside are made by the vacuum evaporation method. The reference samples are also prepared in similar procedures except the annealing step, where there is no Si-QD in the structures.

AFM is used to characterize the size and the distribution of the Si-QD array in the sample. Figure 1 is a plane-view AFM image of the Si-QD array after the gate SiO_2 layer having been removed by diluted HF solution. As shown in the image the shape of Si-QD is roughly spherical and the mean diameter is 6 nm with the deviation less than 10%. The density of the Si-QD is estimated to be $5\times10^{11}/\text{cm}^2$.

The *I-V* characteristics are measured by using HP4156C precision semiconductor parameter analyzer, while the *C-V* characteristics by using HP4294A precision impedance analyzer. Both are carried out at room temperature.

RESULTS AND DISCUSSIONS

A typical current-voltage characteristic is shown in Fig. 2(a). At a glance, the most remarkable feature is the "sharp-edged platformlike" peak structure, which is superposed on the background current (indicated as a dashed base line). According to the peaks' positions in voltage, they could be divided into two regions, with the first two peaks as region 1 [ground state (GS)], and the last six peaks as region 2 [first excited state (FES)]. Apparently, the characteristic is different from the staircases and the peaks observed in the *I-V* characteristics of single quantum dot cases.[15,16] The spacing between the peaks (ΔV_{peak}) in the same region is about 60 mV, while the spacing between the regions (ΔV_{region}) is about 140 mV. Like the peak structure observed in the *I-V* characteristic from a single QD,[15,16] we also consider that it results from the CB and QC effects in the QD array, and assign the spacing ΔV_{peak} and ΔV_{region} in voltage to the CB and QC energies, respectively, which will be discussed later.

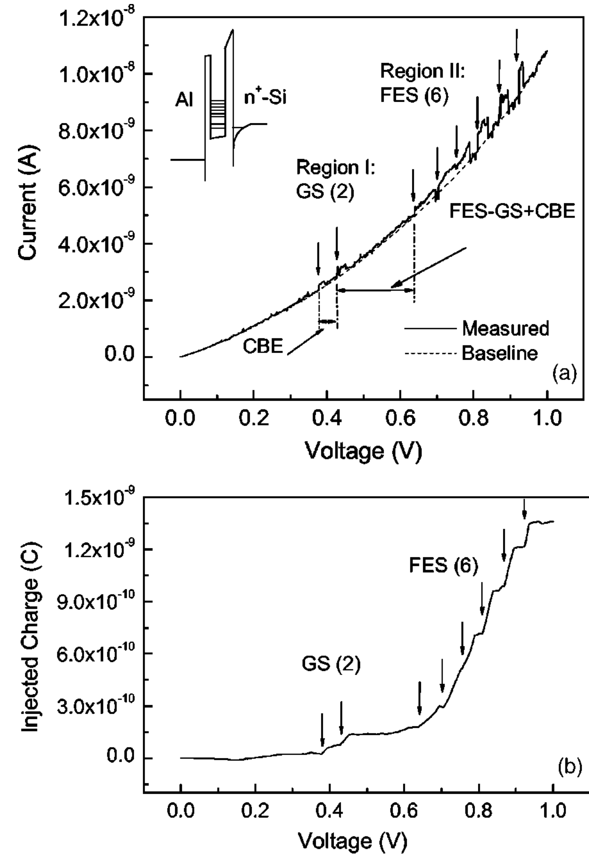

FIG. 2. (a) A typical *I-V* curve with sharp-edged platformlike peaks, which are divided into two regions according to their positions in voltage. The schematic band diagram is shown in the top-left inset. (b) The accumulative injected charges as a function of the voltage ramping.

In comparison, we found that the typical *I-V* curve of the reference sample shows no peak structure, which leads us to attribute the peak structure to the electrons' resonant tunneling into the well-defined Si-QD array.

Further investigations of the unique peak structure disclose another two noticeable features: (i) The peak's area S_{peak}, obtained by integrating each peak after subtracting the base line, keeps nearly constant especially for those in the same region and (ii) the conductance increment ΔG for each peak, associated with an extra charging current, shows to be quantized. The related data are listed in Table. I.

The energy band diagram is shown schematically in the top-left inset of Fig. 2(a), corresponding to the situation of positive bias. It is worth to note that, due to the different oxidation rates of *a*-Si and nc-Si, as mentioned in our fabrication procedure, the gate barrier's thickness is not uniform and the effective thickness is much thinner than that of the tunneling barrier. This situation leads to a situation that the applied voltage bias is mainly dropped on the tunneling barrier and the QDs.

To analyze the above experimental results, we first estimate the effect of weakly interdot coupling among the Si-QD array. The dominant effect is to introduce a tunneling matrix element *t*, between equivalent single-particle states in nearest-neighbor QDs.[18] This is the usual tight-binding ap-

TABLE I. The list of experiment data of the platformlike peaks: the onset position, V_{peak}; the spacing between peaks in the same region, ΔV_{peak} the spacing between the two regions, ΔV_{region}; the current jump at the onset of each peak, ΔI_{jump}; and calculated results, the injected charge for each peak, $Q_{charged}$; and the conductance increment at the onset of each peak, ΔG_{charge}.

Confinement levels	GS (2)		FES (6)					
Peak no.	1	2	1	2	3	4	5	6
V_{peak} (V)	0.38	0.43	0.64	0.70	0.76	0.81	0.87	0.93
ΔV_{peak} (V)		0.05		0.06	0.06	0.05	0.06	0.06
ΔV_{region} (V)			0.14					
$Q_{charged}$ (10^{-11} C)	4.1	5.6	20	23.7	22.5	22.5	20	12.5
ΔI_{jump} (10^{-10} A)	2.0	2.3	3.1	3.6	3.7	7.9	8.5	9.0
ΔG_{charge} (10^{-10} mhos/cm)	5.3	5.3	4.8	4.9	4.7	9.5	9.8	9.8

proximation and justified when t is not too large. The matrix element t between nearest-neighboring QDs is estimated by $t \approx \hbar^2/m^* d^2$, with d as the averaged distance between the QDs and m^* as the effective mass of electron. In our case, the averaged distance d is about 10 nm, thus the t is estimated to be about 3 meV, which is much less than the CB and QC energies in QDs. So, the single particle spectrum in individual Si-QDs can still remain because the interdot coupling is weak compared with energy level separations. Thus, the CB and QC energies can be directly extracted from the peak structure.

The CB energy is estimated according to a semiclassical constant-interaction (CI) theory.[1] For Si-QDs (average diameter of 6 mm) floating above the silicon substrate, their mutual capacitance with the substrate is estimated to be

$$C_{QDs} = 4\pi \cdot \varepsilon_0 \cdot \varepsilon_{\mathrm{SiO_2}} R \cdot \left[\frac{2d}{2d-R} + \frac{R^4}{4d^2(2d-R)^2} \right] = 2 \cdot 10^{-18} F, \quad (1)$$

with R as the radius of the Si-QD and d as the distance between the center of the dot and the substrate surface, that is the oxide thickness of tunneling barrier plus R. The corresponding CB energy reads

$$E_{CB} = \frac{q^2}{C_{QDs}} = 80 \text{ meV}, \quad (2)$$

with q as the elementary charge.

For the quantum confinement, an infinite spherical square well model is employed to approximately estimate the energy spacing of GS and FES, with the effective mass of electron in silicon $0.26 m_0$, where m_0 is the electron rest mass. The formula reads $E_{n,l} = \hbar^2/(2 \cdot m_{\mathrm{Si}} \cdot R_{QDs}^2) \cdot \chi_{n,l}^2$, where $\chi_{n,l}$ is the nth zero point of the spherical Bessel function $j_l(r)$. Then, the energy interval between GS and FES is estimated to be $\Delta E_{QC} = E_{2,0} - E_{1,0} = 160$ meV. From the above calculations, the theoretical results are in good agreement with the experimental results (ΔE_{CB}, 60 meV and ΔE_{QC}, 140 meV), which are listed in Table I.

Based on the discussion above, we further investigate the influences of the interdot coupling. As predicted theoretically, the weak coupling between the equivalent single particle states in individual QDs give rise to a series of corresponding subbands,[18,19,22] with the NOS of each subband equal to the number of the QDs involved in the coupling.[22] In our case, it is roughly the coupled QDs underlying the electrode. Each "platformlike" peak in the *I-V* characteristic originates from a collective single electron charging process, in which electrons are injected into the subband until it is fully filled, thus the amount of injected charge $Q_{charged}$ for each peak can be readily related to the NOS of each subband by $Q_{charged} = q \cdot \mathrm{NOS}$.

To examine the assumption, we first calculate the injected charges $Q_{charged}$ for each peak in the *I-V* characteristic from the peak's underlying area S_{peak}, with the relations as

$$Q_{charged} = \int I_{charge} \cdot dt = \int I_{charge} \cdot dV \cdot \frac{dt}{dV} = S_{peak} / \left(\frac{dV}{dt} \right)_{const}, \quad (3)$$

with I_{charge} defined as the charging current for each peak, $I_{charge} = I_{measured} - I_{baseline}$, $(dV/dt)_{\mathrm{const}}$ as the voltage ramping rate, which is fixed to 80 mV/s during the *I-V* measurements. The injected charges (Q_{charge}) deduced from S_{peak} for each peak are of the order of 10^{-11} C, and are listed in Table I.

On the other hand, the injected charges $Q_{charged}$ can also be deduced directly from the number of the coupled QDs underlying the electrode, that is, from the density of QDs array and electrode area

$$Q_{charged} = q \cdot \mathrm{NOS} = q \cdot N_{density} \cdot S_{electrode}, \quad (4)$$

with the density of QDs $N_{density} = 5 \times 10^{11}/\mathrm{cm}^2$, and electrode area $S_{electrode} = 0.8 \times 10^{-3}$ cm^2, thus the $Q_{charged}$ is estimated to be 6×10^{-11} C. Compared with the Q_{charge} deduced from S_{peak} (in the order of 10^{-11} C), they are found to be of the same order of magnitude, especially for the first two peaks in GS. This agreement directly indicates that each peak in the *I-V* characteristics corresponds to a collective single electron charging process of large numbers of Si-QDs into subband structure in the Si-QD array.

To give a more straightforward view of the amount of total injected charges, the accumulative injected charges Q_{charge} as a function of the ramping voltage is illustrated in

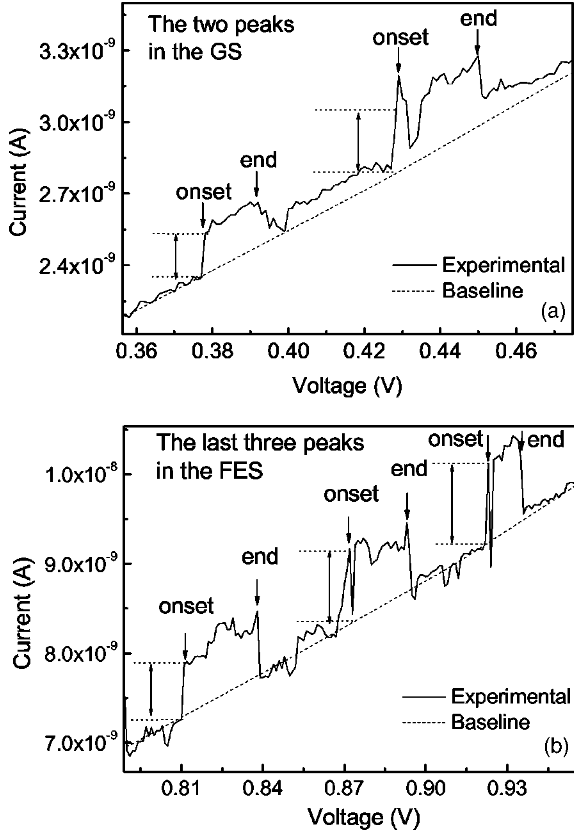

FIG. 3. The details of the peak structure, (a) for the two peaks in region I and (b) for last three peaks in region II. Each peak has an abrupt current jump (ΔI_{jump}, listed in Table I) at the "onset" and a sustaining charging current until an abrupt current drop at the "end."

Fig. 2(b), showing obvious staircases corresponding to the onset of peaks.

In addition, we also study the current jumps at each onset of the platformlike peaks as shown in Fig. 3. From the point of view of conductance, when the Fermi energy level in emitter (substrate) is leveled with the one of the subbands in the Si-QD array, a "resonant tunneling channel" opens and contributes an increment of conductance by

$$\Delta G_{charge} = \frac{\Delta I_{charge}}{V}, \tag{5}$$

where $\Delta G_{charge}=G_{measured}-G_{base\ line}$. According to the configurations of our sample, the conductance quantum is estimated to be $\Delta G_{theoretical}=T\cdot 2e^2/h \approx 10^{-10}$ mhos/cm, in which T stands for the transmission probability for electrons to tunnel through the SiO_2 barrier (2 nm) and is estimated to be the order of 10^{-5} according to WKB approximation. The $\Delta G_{theoretical}$ agrees with the ΔG_{charge} obtained from the experiments as listed in Table I at least in the order of magnitude. Note that the average ΔG_{charge} for the first five platforms is 5.0×10^{-10} mhos/cm, while that of the last three is 9.7×10^{-10} mhos/cm.

On the basis of the analysis above, why we get this unique *I-V* characteristic instead of other types reported in the cases of single QD lies that: the platformlike peak structure actually result from a collective behavior of single electron effects in the Si-QD array. So, the charging current I_{charge}, which is limited by the conductance quantum, has to last for a moment Δt [reflected as ΔV of the width of the peaks, $\Delta V=\Delta t\cdot(dV/dt)_{const}$] to supply enough electrons for all the QDs involved in the formation of this subband, that is the NOS of the subbands.

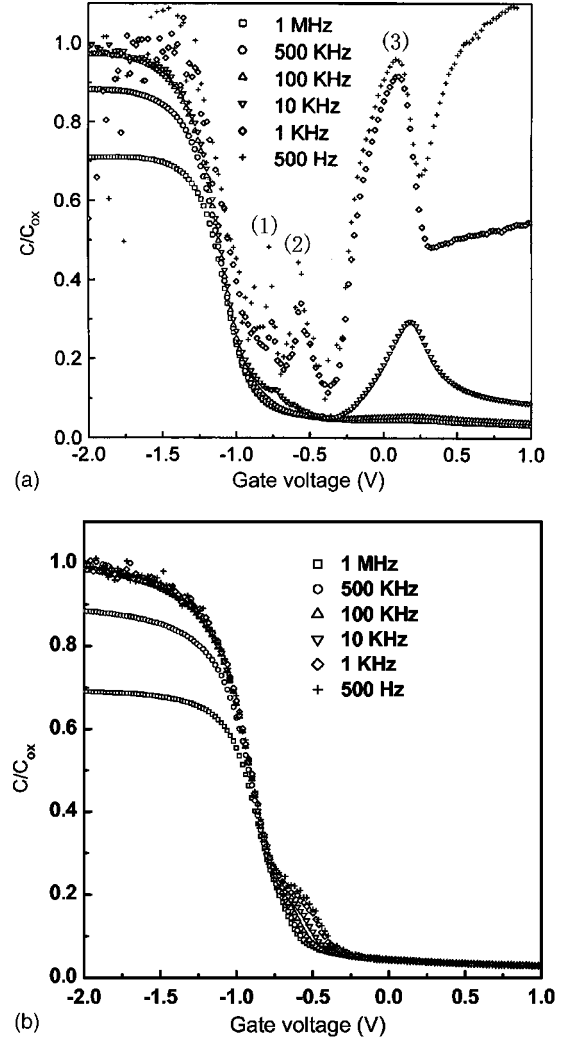

FIG. 4. Frequency-dependent *C-V* characteristics of (a) the sample (annealed) with well-defined Si-QDs measured at different ac frequencies, in which discrete capacitance peaks are observed; (b) the reference sample (unannealed) measured at different ac frequencies, in which no peaks but a shoulder are observed.

More experiment evidence is the results of the *C-V* measurement of a similar structure (except that the substrate is *p*-Si), which is investigated with different frequencies at room temperature. As shown in Fig. 4(a), three remarkable capacitance peaks are observed in the *C-V* characteristics at low frequencies. Thus, according to the analysis in our previous reports,[23] the first two capacitance peaks correspond to the resonance response with the GS in QDs, while the third peak corresponds to the FES, respectively. The energy spacing ΔE_{CB} can be estimated to be 57 meV from the voltage spacing $(\Delta V_{1,2})$ between the first two capacitance peaks, while the energy spacing ΔE_{QC} between the GS and FES in

QDs, is estimated to be 143 meV. They are in good agreement with that obtained from the peak structure in the *I-V* characteristics.

We also perform the measurements of the frequency-dependent *C-V* characteristics of the reference sample, which is shown in Fig. 4(b). We found that there is no peak structure observed in the curves, but a capacitance shoulder, which is related to the interface states in the structure and discussed in our pervious work.[23] Compared with the annealed sample with well-defined Si-QDs, as shown in Fig. 4(a), it is clear that the capacitance shoulder is greatly reduced while the peak structure appears. Therefore, we can again attribute this peak structure observed in the *C-V* characteristics to the quantum confinement levels in the Si-QDs.

Meanwhile, we can also see that the capacitance peaks tend to decrease with the increase of ac frequencies. This phenomenon has been discussed in detail in our previous work,[23] in brief, it can be attributed to the fact that for higher ac frequencies, electrons in an inversion layer cannot follow the ac modulation to tunnel through the tunneling SiO_2 layer into the Si-QD array; while for lower frequencies, electrons can follow the ac modulation and tunnel through the layer, thus giving rise to the capacitance peaks. Moreover, from the capacitance peak (at lowest frequencies) we can also calculate the injected charges for each peak,[25] on the other hand the charged electrons can also be deduced from the density of the Si-QDs (5×10^{11} obtained directly from the AFM) and the electrode area, given that each Si-QD is charged with only one electron. The results show that they agree well. So, the *C-V* results support again that collective single electron effects can be observed in the Si-QD array at room temperature.

CONCLUSION

In summary, collective single electron effects in the single layer Si-QD array are demonstrated at room temperature, with direct observation of collective Coulomb blockade and quantum confinement effects both in the *I-V* characteristics and in the *C-V* characteristics, which differ remarkably from the peaks and the staircases structures reported for the case in individual QDs. Moreover, the experimental results verify our hypothesis that the unique peak structure observed in the characteristics are attributed to the subband structure among the coupled QD array induced by the weak interdot coupling. Thus, the important theoretical and experimental basis has been laid for the single layer QD array's potential applications in the fabrication of nanoelectronic devices.

ACKNOWLEDGMENTS

This work is financially supported by the State Key Program for Basic Research of China (Grant No. 2001CB610503) and National Nature Science Foundation of China (Nos. 90101020, 90301009, and 10174035).

*Author to whom correspondence should be addressed. Email address: kjchen@netra.nju.edu.cn

[1] D. K. Ferrey and S. M. Goodnick, *Transport in Nanostructures* (Cambridge University Press, Cambridge, U.K., 1997), Chaps. 2–7.
[2] M. A. Kastner, Rev. Mod. Phys. **64**, 849 (1992).
[3] M. A. Reed, J. N. Randall, R. J. Aggarwal, R. J. Matyi, T. M. Moore, and A. E. Wetsel, Phys. Rev. Lett. **60**, 535 (1988).
[4] M. A. Kastner, Int. J. High Speed Electron. Syst. **12**, 163 (2002).
[5] D. V. Averin, A. N. Korotkov, and K. K. Likharev, Phys. Rev. B **44**, 6199 (1991).
[6] Y. Ito, T. Hatano, A. Nakajima, and S. Yokoyama, Appl. Phys. Lett. **80**, 4617 (2002).
[7] W. Wu, J. Gu, H. Ge, C. Keimel, and S. Y. Chou, Appl. Phys. Lett. **83**, 2268 (2003).
[8] L. J. Guo, E. Leobandung, and S. Y. Chou, Science **275**, 649 (1997).
[9] K. Yano, T. Ishii, T. Sano, T. Mine, F. Murai, T. Hashimoto, T. Kobayashi, T. Kure, and K. Seki, Proc. IEEE **87**, 633 (1999).
[10] A. N. Korotkov, J. Appl. Phys. **92**, 7291 (2002).
[11] H. Ishikuro and T. Hiramoto, Appl. Phys. Lett. **71**, 3691 (1997).
[12] B. H. Choi, S. W. Hwang, I. G. Kim, H. C. Shin, Y. Kim, and E. K. Kim, Appl. Phys. Lett. **73**, 3129 (1998).
[13] D. N. Kouvatsos, V. Ioannou-Sougleridis, and A. G. Nassiopoulou, Appl. Phys. Lett. **82**, 397 (2003).
[14] S. Tiwari, F. Rana, H. Hanafi, A. Hartstein, E. F. Crabbe, and K. Chan, Appl. Phys. Lett. **68**, 1377 (1996).
[15] T. Baron, P. Gentile, N. Magnea, and P. Mur, Appl. Phys. Lett. **79**, 1175 (2001).
[16] M. Fukuda, K. Nakaga, S. Miyazaki, and M. Hirose, Appl. Phys. Lett. **70**, 2291 (1997).
[17] C. Wasshuber, H. Kosian, and S. Selberherr, IEEE Trans. Comput.-Aided Des. **16**, 937 (1997).
[18] C. A. Stafford and S. Das Sarma, Phys. Rev. Lett. **72**, 3590 (1994).
[19] D. M. Kou, G. Y. Guo, and Yia-Chung Chang, Appl. Phys. Lett. **79**, 3851 (2001).
[20] W. G. van der Wiel, S. de Francheschi, J. M. Elzerman, T. Fujisawa, S. Tarucha, and L. P. Kouwenhoven, Rev. Mod. Phys. **75**, 1 (2003).
[21] V. Moldoveanu, A. Aldea, and B. Tanatar, Phys. Rev. B **70**, 085303-1 (2004).
[22] L. P. Kouwenhoven, F. W. J. Hekking, B. J. van Wees, and C. J. P. M. Harmans, C. E. Timmering, and C. T. Foxon, Phys. Rev. Lett. **65**, 361 (1990).
[23] J. Shi, L. Wu, X. Huang, J. Liu, Z. Ma, W. Li, X. Li, J. Xu, D. Wu, A. Li, and K. Chen, Solid State Commun. **123**, 437 (2002).
[24] L. Zhang, K. Chen, L. Wang, W. Li, J. Xu, X. Huang, and K. Chen, J. Phys.: Condens. Matter **14**, 10083 (2002).
[25] G. Medeiros-Ribeiro, D. Leonard, and P. M. Petroff, Appl. Phys. Lett. **66**, 1767 (1995).